NACA RM L51G06

NACA

RESEARCH MEMORANDUM

DAMPING IN ROLL OF ROCKET-POWERED TEST VEHICLES HAVING SWEPT, TAPERED WINGS OF LOW ASPECT RATIO

By E. Claude Sanders, Jr., and James L. Edmondson

Langley Aeronautical Laboratory
Langley Field, Va.

NATIONAL ADVISORY COMMITTEE
FOR AERONAUTICS

WASHINGTON
October 8, 1951

E R R A T U M

NACA RM L51G06

DAMPING IN ROLL OF ROCKET-POWERED TEST VEHICLES HAVING SWEPT, TAPERED WINGS OF LOW ASPECT RATIO

By E. Claude Sanders, Jr., and James L. Edmondson

October 8, 1951

Page 10: Reference 5 should be extended to include a second publication providing for a theoretical method applying to wings with both supersonic leading and trailing edges. The citation given for this reference should therefore be corrected as follows:

5. (a) Malvestuto, Frank S., Jr., Margolis, Kenneth, and Ribner, Herbert S.: Theoretical Lift and Damping in Roll at Supersonic Speeds of Thin Sweptback Tapered Wings with Streamwise Tips, Subsonic Leading Edges and Supersonic Trailing Edges. NACA Rep. 970, 1950.

(b) Harmon, Sidney M., and Jeffreys, Isabella: Theoretical Lift and Damping in Roll of Thin Wings with Arbitrary Sweep and Taper at Supersonic Speeds. Supersonic Leading and Trailing Edges. NACA TN 2114, 1950.

NACA RM L51G06

NATIONAL ADVISORY COMMITTEE FOR AERONAUTICS

RESEARCH MEMORANDUM

DAMPING IN ROLL OF ROCKET-POWERED TEST VEHICLES HAVING SWEPT, TAPERED WINGS OF LOW ASPECT RATIO

By E. Claude Sanders, Jr., and James L. Edmondson

SUMMARY

Flight tests of rocket-powered models have been conducted to determine the damping in roll of a group of swept, tapered wings designed for flight in the transonic speed region. The Mach number range of these tests was from approximately 0.7 to 1.4. The experimental damping in roll for all configurations was less than predicted by linearized theory throughout the Mach number range of these tests. The only wing in this group that experienced an appreciable transonic lateral trim change was the one with a 7-percent-thick circular-arc airfoil section. The magnitude of this trim change was diminished by the addition of half-slab ailerons.

INTRODUCTION

The damping in roll of wing configurations is of importance in the calculation of lateral stability and rolling performance of airplanes and missiles. The National Advisory Committee for Aeronautics has devised a simplified rocket-model technique, reference 1, utilizing a canted nozzle to provide a torque, which allows a determination of damping in roll at high-subsonic, transonic, and supersonic speeds at high Reynolds numbers. This technique also yields data on lateral trim changes in the transonic range and the total drag. As a part of the program of wings investigated with this technique, a series of swept, tapered wings of aspect ratios from 2.9 to 6.0, considered suitable for transonic aircraft and related only by their purpose, has been investigated and the results are presented herein.

The various wing plan forms were mounted in a three-wing arrangement on identical fuselages and were flown through a Mach number range of approximately 0.7 to 1.4 corresponding to a Reynolds number range of 2.5×10^6 to 8.3×10^6 based on the mean aerodynamic chord. The

flight tests were conducted at the Pilotless Aircraft Research Station at Wallops Island, Va.

SYMBOLS

C_l	rolling-moment coefficient (L/qSb)
C_{l_p}	damping-in-roll derivative $\left(\frac{\partial C_l}{\partial \frac{pb}{2V}}\right)$
C_D	total-drag coefficient (D/qS)
D	total drag, pounds
L	rolling moment, foot-pounds
L_o	out-of-trim rolling moment, foot-pounds (produced by constructional inaccuracies)
T	torque, pound-feet
p	rolling angular velocity, radians per second
$\dot{p}$	rolling angular acceleration, radians per second^2
V	forward velocity, feet per second
q	dynamic pressure, pounds per square foot
M	Mach number
A	aspect ratio (b^2/S')
R	Reynolds number, based on mean aerodynamic chord
λ	taper ratio, ratio of tip chord to chord at body center line
t/c	airfoil-section thickness ratio (parallel to center line)
Λ	angle of sweep of wing leading edge, degrees
b	wing span, feet (diameter of circle generated by wing tips)
S'	twice area of one wing, square feet (wing assumed to extend to model center line)

S thrice area of one wing

I_X moment of inertia about longitudinal axis, slug-feet^2

M_θ wing torsional stiffness, inch-pounds per degree

Subscripts:

1 sustainer-on flight

2 coasting flight

MODELS AND APPARATUS

The models flown in this investigation consisted of identical bodies fabricated from wood and equipped with canted nozzles, spinsonde nose sections, and with three equally spaced wings mounted near the rear of the bodies (see fig. 1). The three types of wing construction used are also shown in figure 1.

The various wing configurations investigated are shown in figure 2 and a tabulation of the pertinent wing geometry is presented in table I. Wing 1b was identical to wing 1a with the exception of undeflected, 20-percent-chord, half-slab ailerons which were installed on each wing semispan as may be seen in figure 2. The trailing-edge thickness of the half-slab aileron was one-half the aileron thickness at the hinge line. Wing 2a and wing 2b differ only in airfoil section. Figure 3 contains photographs of two of the models tested.

The models were launched from a rail-type launcher at an elevation angle of 70° to the horizontal, and were boosted to a Mach number of approximately 0.7 by means of a booster rocket, and allowed to separate; then the models were accelerated by an internal rocket motor to a Mach number of from 1.2 to 1.4. Thus, a Mach number range from approximately 0.7 to 1.4 was covered corresponding to a Reynolds number of from 2.5×10^6 to 8.3×10^6 based on the mean aerodynamic chord of the wing.

The rate of roll and rolling acceleration were obtained by means of modified spinsonde (reference 2) contained in the nose of the model. The flight-path velocity and longitudinal acceleration were recorded with a doppler velocimeter. Atmospheric measurements covering the altitude range of the flight test were obtained with radiosondes.

REDUCTION OF DATA

The damping-in-roll derivative was calculated by balancing of the moments acting on the model. The torque nozzle and wing misalinement produced rolling moments which were balanced by the inertia moment and the damping moment produced by the wing and body. Moment equilibrium for one degree of freedom may be written:

$$I_X\dot{p} - \frac{\partial L}{\partial p} p = T + L_o \tag{1}$$

Converting equation (1) into coefficient form at the same Mach number for the accelerated and the decelerated portion of flight and solving the two resulting equations simultaneously for the damping-in-roll derivatives yields:

$$-C_{l_p} = \frac{\frac{T}{q_1} - \left(I_{X_1}\dot{p}_1 - I_{X_2}\dot{p}_2\right)}{\frac{Sb^2}{2}\left(\frac{p_1}{V_1} - \frac{p_2}{V_2}\right)} \tag{2}$$

The complete analysis of this method for determining the damping in roll derivatives may be found in reference 1.

The accuracy of C_{l_p}, C_D, and their component errors for these tests are estimated to be within the following limits:

Torque, T, lb-ft	±2.50
Rolling angular velocity, radians/sec	±1.00
Damping-in-roll derivative, C_{l_p}	±0.03
Total-drag coefficient, C_D	±0.002
Mach number, M	±0.010

The preceding estimations are based on individual model calculations; however, the relative magnitudes of the lateral trim changes of duplicate models may affect the repeatability of p and, consequently, C_{l_p} throughout the Mach numbers at which this trim change is effective. A more complete analysis of factors producing the error in C_{l_p} is reported in reference 1.

RESULTS AND DISCUSSION

Two identical models were flown for each wing configuration to allow for instrument and recording failures. One model each with wings 1a, 2a, 3, and 8 resulted in incomplete records and therefore no damping-in-roll or lateral-trim-change data; however, drag data were obtained for the models with wings 1a and 3. At least one complete set of data for each configuration was obtained and is presented herein with one exception: the drag data for the model with wing 2b were questionable and were therefore omitted.

Rolling velocity and drag are presented for each individual model, but an average value of the experimental damping-in-roll derivative is shown for each pair of models for comparison with theoretical data. The maximum deviation from this average value for any particular model is 6 percent.

Damping in Roll

The experimental damping-in-roll derivatives and the appropriate linearized theory for each wing configuration are plotted against Mach number in figure 4. A comparison of these data indicates a tendency for experimental values of C_{l_p} to be lower than theoretical values of C_{l_p}. This tendency, which has been noticed in a previous investigation of damping-in-roll characteristics of other wing plan forms (reference 1), is believed to be due to the combined effects of section thickness, body influence, mutual interference effects between wings, and wing twisting which was not taken into consideration in the theory for isolated wings (references 3, 4, 5, and 6).

Comparative values of torsional stiffness for each wing are presented in table I. The wing was loaded about the midspan and the twist was measured at the wing tip. The technique used is explained in reference 7; however, no corrections for torsional stiffness have been applied in this paper.

It is apparent from a comparison of the data of wing 1a with wing 1b (fig. 5(a)) that the damping in roll from this technique varies with the magnitude of the lateral trim change. It is also evident from figure 4(a) that the undeflected half-slab ailerons increase the damping in roll through the speed range tested.

A comparison of the data for a 36.5° swept wing (wing 2a) with the data for a thinner 36.5° swept wing (wing 2b), figure 4(b), shows a reduction in damping in roll due to an increase in maximum thickness

ratio, as shown in reference 8. This is especially evident in the high-subsonic range. The experimental values were much lower than theoretical values of C_{l_p} for both wings in the supersonic range.

It is interesting to note that the hexagonal airfoil (wing 3), figure 4(c), has a higher C_{l_p} than the previously discussed models in the supersonic range and is only lower than the modified circular-arc airfoil (wing 1b) in the subsonic range, although it has a lower aspect ratio. This is believed to be due mainly to a small thickness ratio $\left(4\frac{1}{2} \text{ percent}\right)$, reference 8, difference in airfoil section, reference 9, and smaller leading-edge sweep angle, reference 10.

The damping in roll of the 37.4° swept wing (wing 4) was slightly higher than for the 46.7° swept wing (wing 5), figure 4(d). The difference in their damping in roll was about the same as that predicted by theory. These wings were also tested in the Langley 7- by 10-foot tunnel transonic bump (reference 10). The damping-in-roll data obtained by this method were higher than the data obtained from the torque-nozzle technique, but the difference in C_{l_p} due to sweep for the two wings was approximately the same for both techniques.

The experimental damping in roll of the 60.9° swept wing (wing 6) is also shown in figure 4(d). Although wing 6 has a larger leading-edge sweep than does wing 4 or 5, which would lower the C_{l_p}, the difference in experimental data for wing 6 as compared with wing 4 or 5 is much greater than predicted by theory. The difference in flexibility may account for a portion of the difference in C_{l_p}.

The values of C_{l_p} for wing 7, swept 63°, figure 4(e) and wing 8, swept 46.2°, figure 4(f), are lower than predicted by theory.

In an attempt to account for the difference between experimental and theoretical values of C_{l_p} for these wings, an empirical correction factor (reference 8) developed for rectangular wings was applied to existing theory. This factor, which is dependent upon the wing thickness and aspect ratio, is expressed as $\left(1 - \frac{t}{c}\right)^{\frac{2}{3}A}$ and is multiplied by values from approximate theory. Although the limits of operation for this factor are not known, the corrected theoretical values were in good agreement with the experimental values of C_{l_p} in the subsonic region but remained higher than experimental values of C_{l_p} in the supersonic region. It can be seen that the more flexible wings have the greatest difference between experimental and theoretical values of C_{l_p}.

This seems to indicate that theory will have to be further modified to include aeroelastic effects.

Lateral Trim Change

The lateral trim change through the transonic-speed region can be observed in figure 5, which is a plot of the rolling velocity during coasting flight as a function of Mach number. Only the coasting flight is shown because this condition contains no external disturbing forces and allows a more accurate determination of the trim change; however, all models which experienced a trim change during coasting flight also experienced a similar trim change in the presence of the external torque. The difference in rolling velocities for similar models was believed due to wing misalinement. Wing 1a (fig. 5(a)) had a large abrupt change in rolling velocity through the transonic region; wing 1b had only a small change. This tends to indicate that the half-slab ailerons on wing 1b retarded flow separation from the surface of the wing, thereby decreasing the severity of the lateral trim change through the transonic region. None of the remaining models had a lateral trim change in the critical Mach number range.

Drag

The variations of total drag coefficient at zero lift with Mach number obtained from these tests are presented in figure 6. There was good agreement in all cases between identical models.

The area of all wings, except 4 and 5, was within ±3 percent of the mean area, which allows a direct comparison of their drag coefficients. Although the body drag through this Mach number range has not been accurately determined, the contribution of the body drag to the total drag will be approximately the same in these cases. The areas of wings 4 and 5 were approximately 60 percent greater and would result in the contribution of the body drag being decreased about 60 percent, yielding a lower C_D than would be suitable for comparison purposes.

It is interesting to note that, although the half-slab aileron increased the damping-in-roll coefficient of wing 1b over that of wing 1a, it had no noticeable effect on the drag characteristics of these wings, as is evident by the good agreement between them, figure 6(a).

Summary of Model Characteristics

The following table contains a list of the wing-body configurations tested and a summary of the damping-in-roll and drag characteristics of each:

Wing	A	Λ (deg)	t/c (parallel to center line)	C_{l_p}		C_D		Drag-rise Mach number	Transonic trim change
				M = 0.8	M = 1.20	M = 0.8	M = 1.2		
1a	4.0	42.7	0.07	0.245	[a]0.245	0.018	0.049	0.90	Yes
1b	4.0	42.7	.07	.264	.295	.020	.049	.90	Yes
2a	3.5	36.5	.10 to .12	[a].202	.230	.020	.058	.88	No
2b	3.5	36.5	.10	.221	.241	-----	-----	----	No
3	2.9	23.1	.045	[a].242	.309	.017	.039	.88	No
4	4.0	37.4	.06	.272	.250	.014	.032	.93	No
5	4.0	46.7	.06	.254	[a].215	.014	.026	.94	No
6	4.0	60.9	.06	.122	.090	.019	.029	.96	No
7	3.5	63.0	.05	------	.150	-----	.027	.97	No
8	6.0	46.2	.09	[a].248	[a].168	.022	.045	.93	No

[a]Curve extrapolated

CONCLUDING REMARKS

These wing plan forms are related only by their purpose and, therefore, do not allow conclusions as to the effect of design parameters except in limited cases. The experimental damping in roll for all configurations was less than predicted by linearized theory throughout the Mach number range of these tests. In general, the thickness-corrected damping-in-roll theory agreed with experimental data at subsonic speeds and was a correction in the right direction at supersonic speeds. The addition of an undeflected half-slab aileron on the 42.7° swept wing (wing 1b) decreased the magnitude of transonic lateral trim change and corresponding change in C_{l_p} and increased damping through the transonic speed range with little penalty in subsonic drag and no noticeable effect on supersonic drag. The effect of the larger tip thickness ratio on the 36.5° swept wing (wing 2a) was a slight decrease in damping. The increase in sweep from 37.4° (wing 4) to 46.7° (wing 5) resulted in less supersonic drag and slightly less damping in roll.

The damping in roll for the 23.1° swept wing (wing 3) was higher in the supersonic range than for the other wings tested. There was no abrupt lateral trim change in the transonic region and the drag was low. This was believed to be largely due to the low thickness ratio $\left(4\frac{1}{2}\text{ percent}\right)$.

The only wings in this swept group to experience an appreciable transonic lateral trim change were the ones with a circular-arc airfoil section.

Langley Aeronautical Laboratory
National Advisory Committee for Aeronautics
Langley Field, Va.

REFERENCES

1. Edmondson, James L., and Sanders, E. Claude, Jr.: A Free-Flight Technique for Measuring Damping in Roll by Use of Rocket-Powered Models and Some Initial Results for Rectangular Wings. NACA RM L9I01, 1949.

2. Harris, Orville R.: Determination of the Rate of Roll of Pilotless Aircraft Research Models by Means of Polarized Ratio Waves. NACA TN 2023, 1950.

3. Bird, John D.: Some Theoretical Low-Speed Span Loading Characteristics of Swept Wings in Roll and Sideslip. NACA Rep. 969, 1950. (Formerly NACA TN 1839.)

4. Polhamus, Edward C.: A Simple Method of Estimating the Subsonic Lift and Damping in Roll of Sweptback Wings. NACA TN 1862, 1949.

5. Malvestuto, Frank S., Jr., Margolis, Kenneth, and Ribner, Herbert S.: Theoretical Lift and Damping in Roll at Supersonic Speeds of Thin Sweptback Tapered Wings with Streamwise Tips, Subsonic Leading Edges, and Supersonic Trailing Edges. NACA Rep. 970, 1950. (Formerly NACA TN 1860.)

6. Walker, Harold J., and Ballantyne, Mary B.: Pressure Distribution and Damping in Steady Roll at Supersonic Mach Numbers of Flat Swept-Back Wings with Subsonic Edges. NACA TN 2047, 1950.

7. Broadbent, E. G., and Woodcock, D. L.: The Measurement of Structural Stiffnesses of Aircraft. R. & M. No. 2208, British A.R.C., 1945.

8. Edmondson, James L.: Damping in Roll of Rectangular Wings of Several Aspect Ratios and NACA 65A-Series Airfoil Sections of Several Thickness Ratios at Transonic and Supersonic Speeds As Determined with Rocket-Powered Models. NACA RM L50E26, 1950.

9. Dietz, Albert E., and Edmondson, James L.: The Damping in Roll of Rocket-Powered Test Vehicles Having Rectangular Wings with NACA 65-006 and Symmetrical Double-Wedge Airfoil Sections of Aspect Ratio 4.5. NACA RM L50B10, 1950.

10. Lockwood, Vernard E.: Effects of Sweep at Transonic Speeds on the Damping-in-Roll Characteristics of Three Sweptback Wings Having an Aspect Ratio of 4. NACA RM L50J19, 1950.

TABLE I

GEOMETRIC CHARACTERISTICS OF WINGS

Wing	Sweep of L.E. (deg)	Aspect ratio	Taper ratio	Airfoil section parallel to center line	Wing area, S (sq ft)		$M\theta_{Av}$ (in.-lb/deg)	Type wing construction (fig. 1)
					Exposed	Total		
1a	42.7	4.0	0.50	0.07 circular arc	2.66	3.44	1745	C
1b	42.7	4.0	0.50	0.07 circular arc (modified)	2.66	3.44	1825	C
2a	36.5	3.5	0.56	Root - NACA 63-010 Tip - NACA 63-012	2.63	3.43	4080	C
2b	36.5	3.5	0.56	NACA 63-010	2.63	3.44	3780	C
3	23.1	2.9	0.41	0.045 hexagonal	2.64	3.62	3375	A
4	37.4	4.0	0.60	NACA 65A006	4.73	5.69	1845	C
5	46.7	4.0	0.60	NACA 65A006	4.73	5.69	1860	C
6	60.9	4.0	0.60	NACA 65A006	2.54	3.26	324	B
7	63.0	3.5	0.25	NACA 65A005	2.64	3.65	765	A
8	46.2	6.0	0.60	NACA 65A009	2.67	3.27	200	A

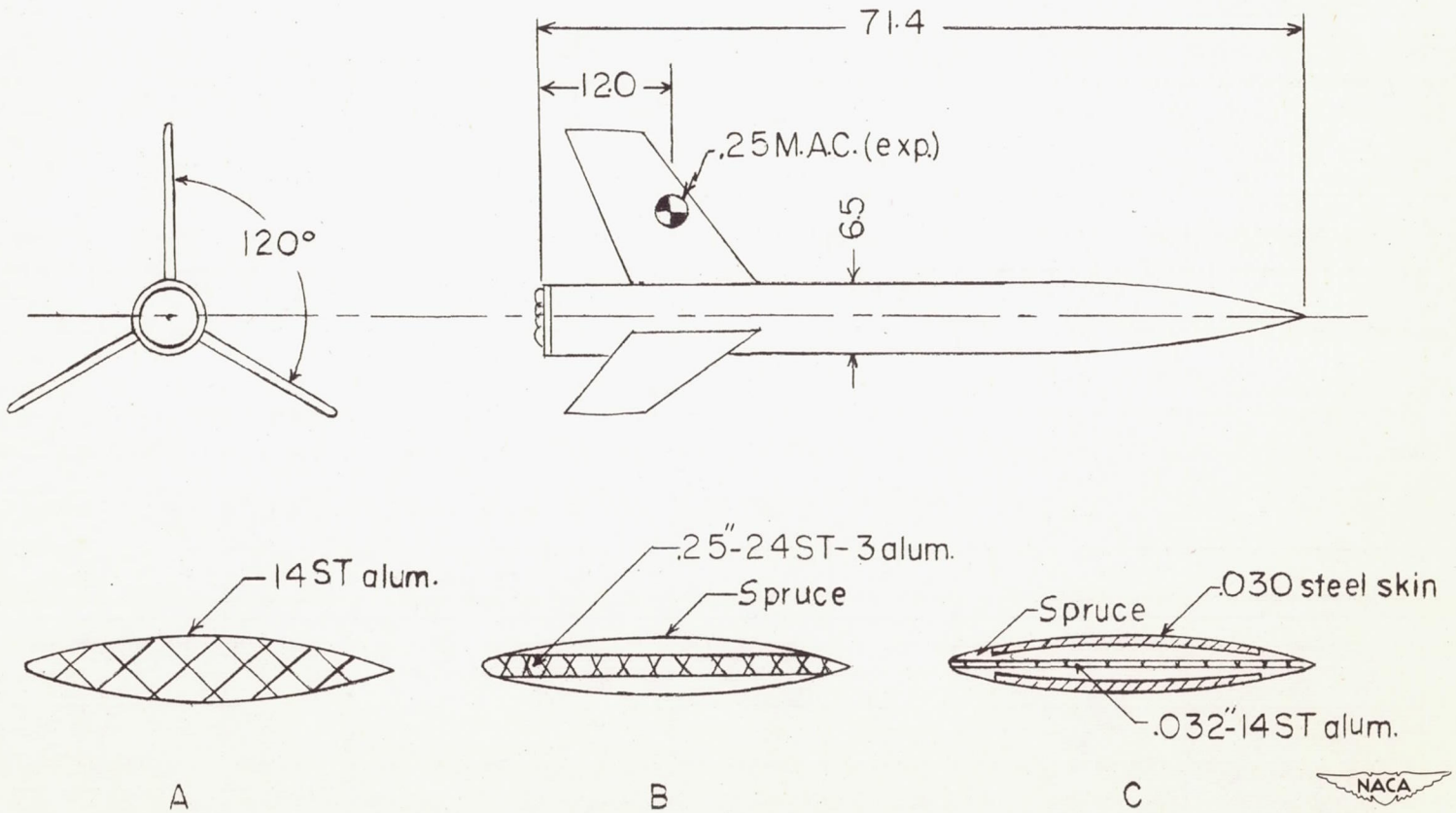

Figure 1.- General arrangement of models and types of wing construction.
All dimensions are in inches.

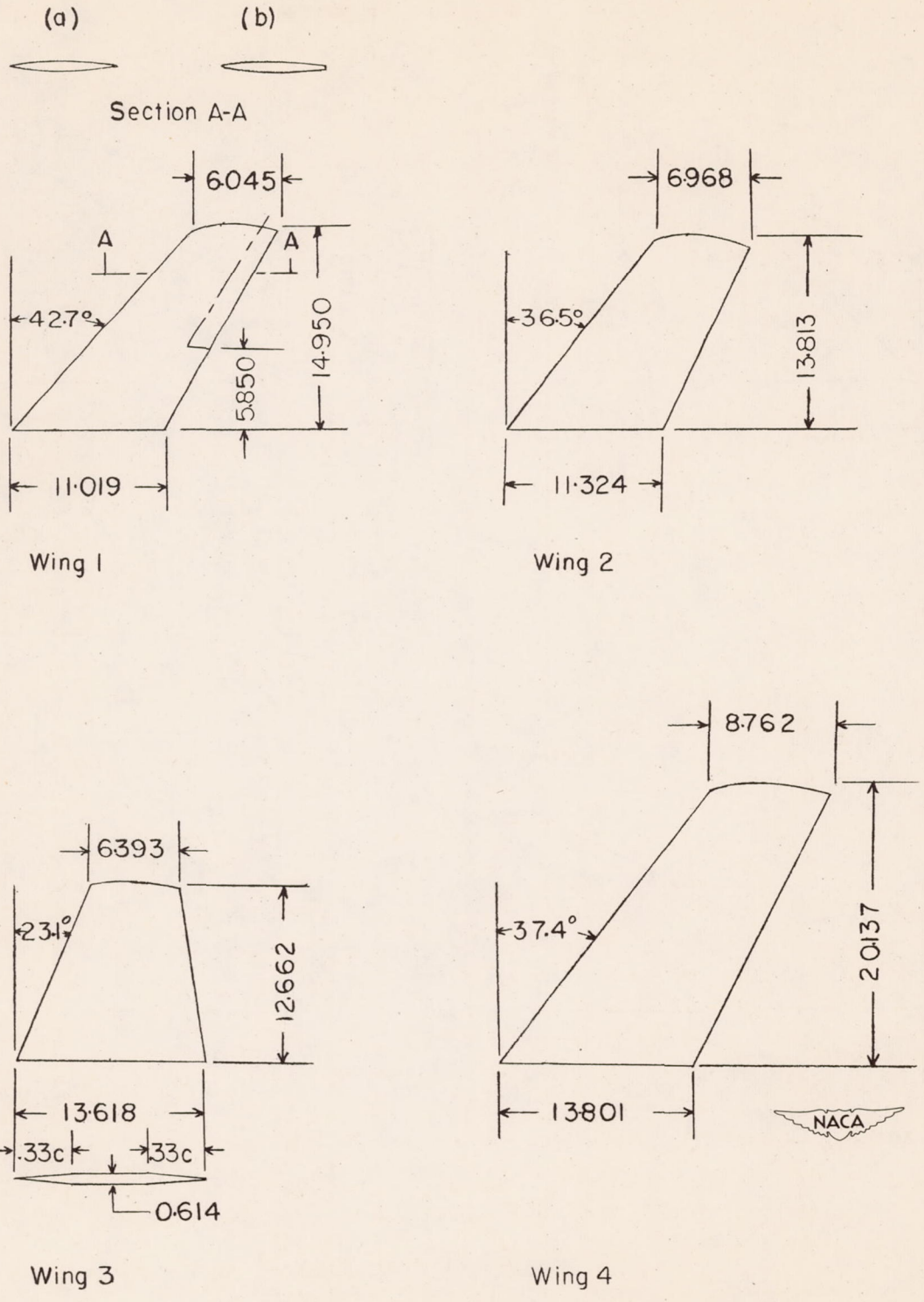

(a) Wings 1 to 4.

Figure 2.- Physical properties of exposed wings. All dimensions are in inches.

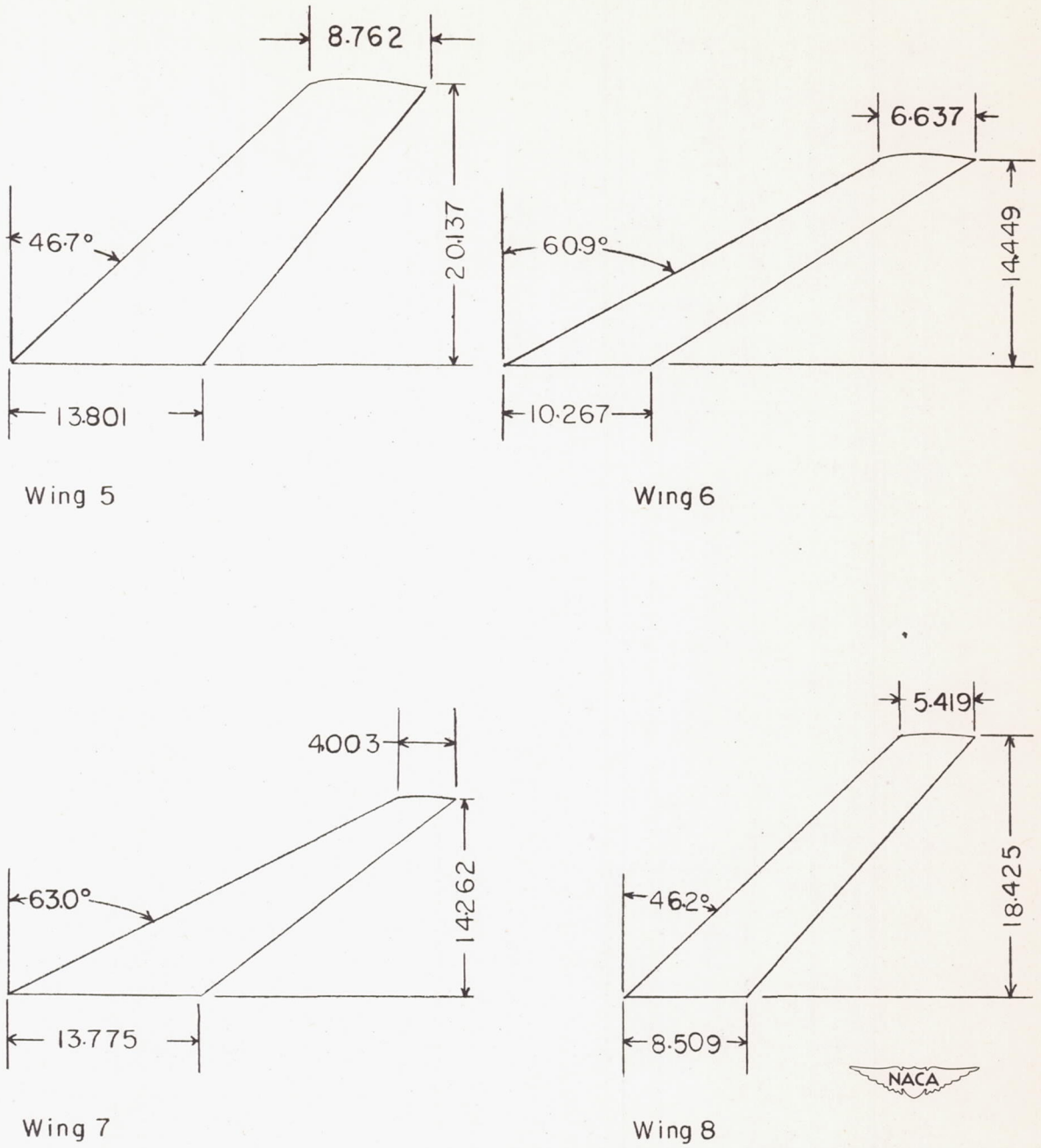

(b) Wings 5 to 8.

Figure 2.- Concluded.

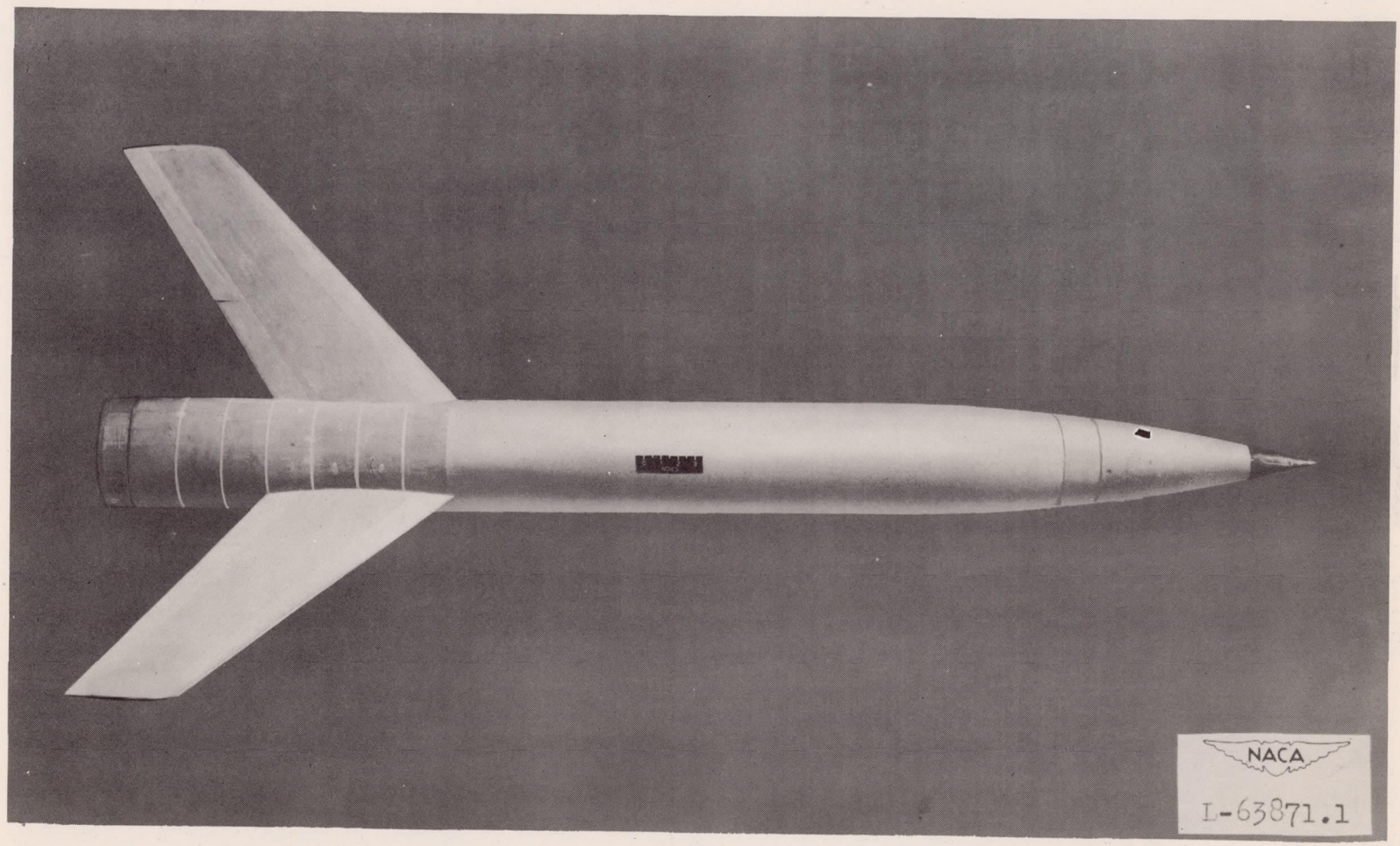

Figure 3.- Photographs of two typical model arrangements tested.

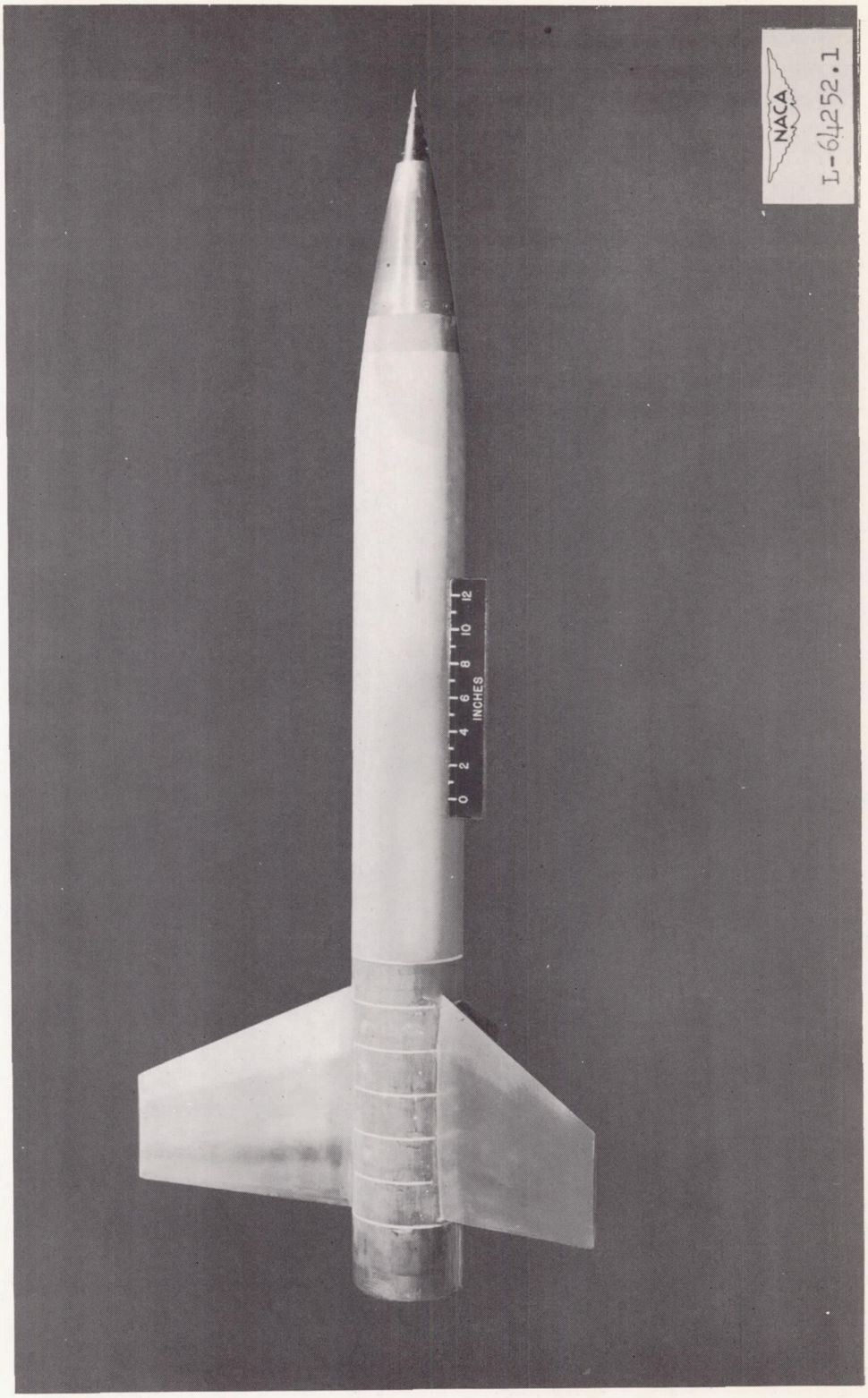

Figure 3.- Concluded.

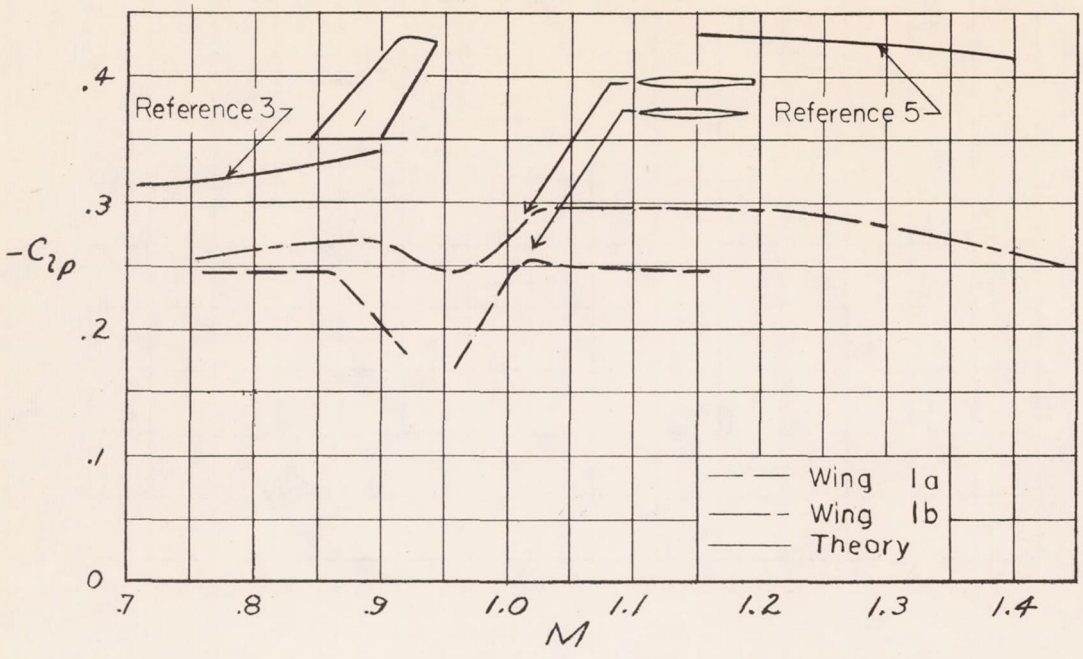

(a) Circular-arc airfoil. $\Lambda = 42.7^{\circ}$.

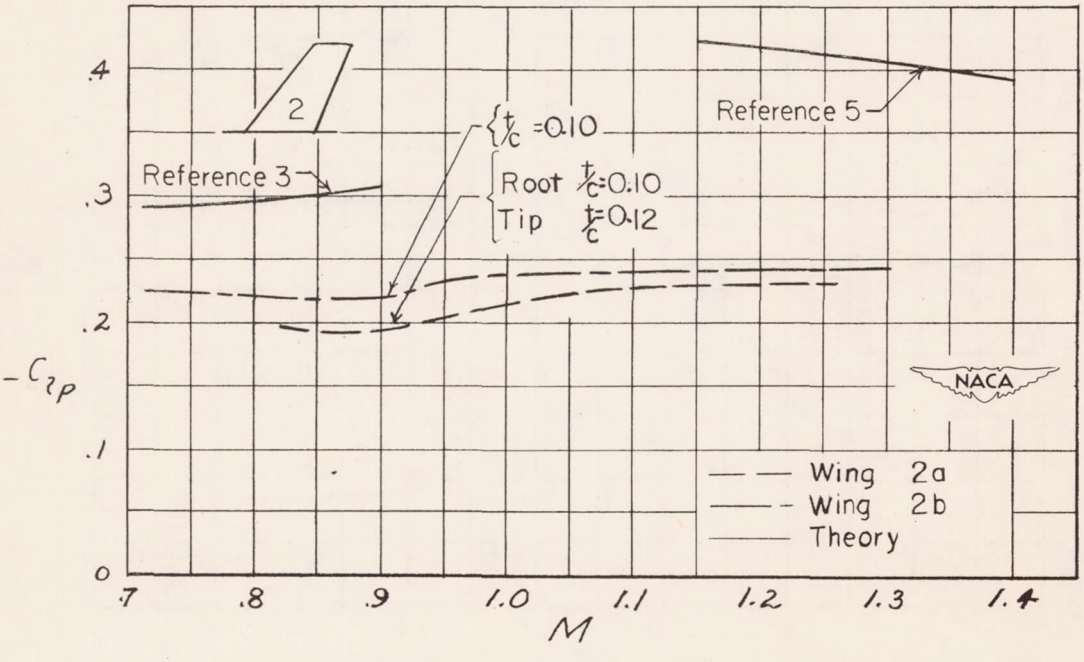

(b) NACA 63-series airfoil. $\Lambda = 36.5^{\circ}$.

Figure 4.- Variation of damping in roll with Mach number.

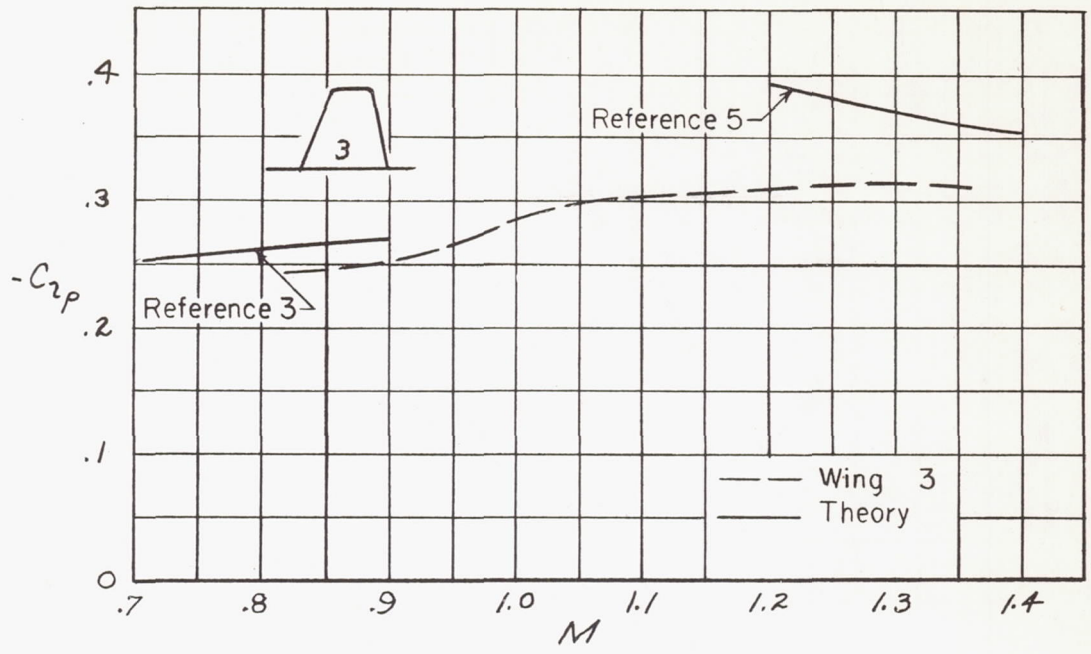

(c) Hexagonal airfoil. $\Lambda = 23.1^{\circ}$.

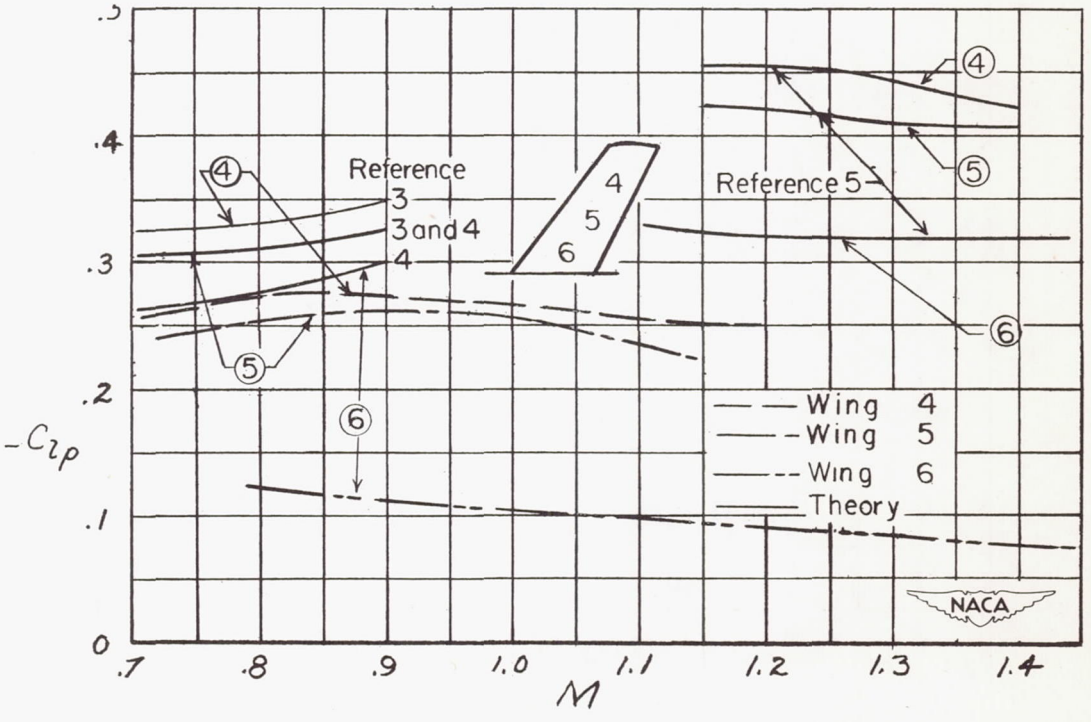

(d) NACA 65A006 airfoil. $\Lambda = 37.4^{\circ}$ (wing 4); $\Lambda = 46.7^{\circ}$ (wing 5); $\Lambda = 60.9^{\circ}$ (wing 6).

Figure 4.- Continued.

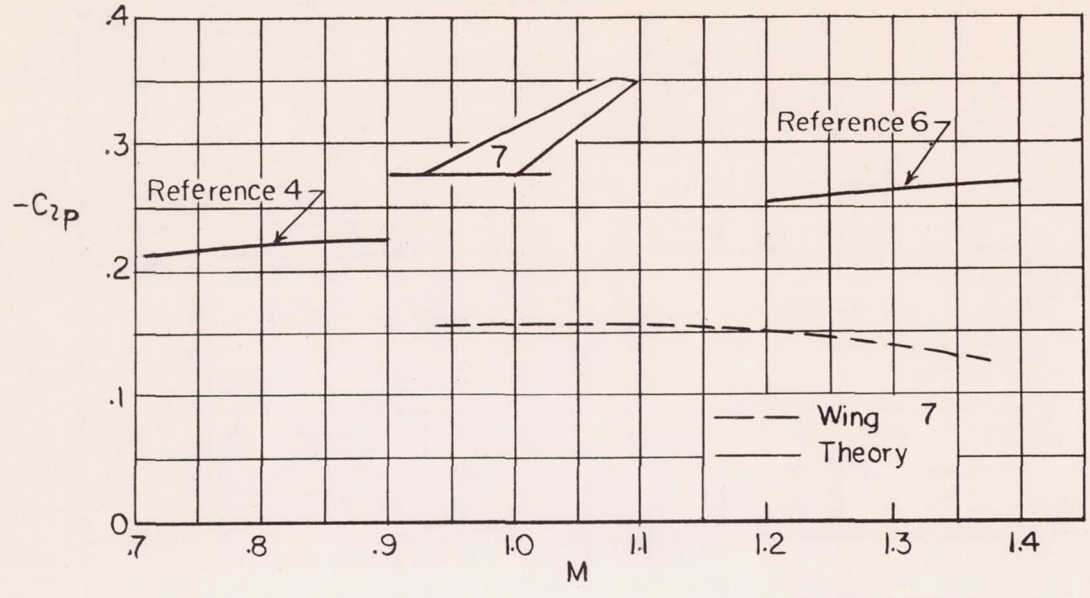

(e) NACA 64A005 airfoil. $\Lambda = 63^{\circ}$.

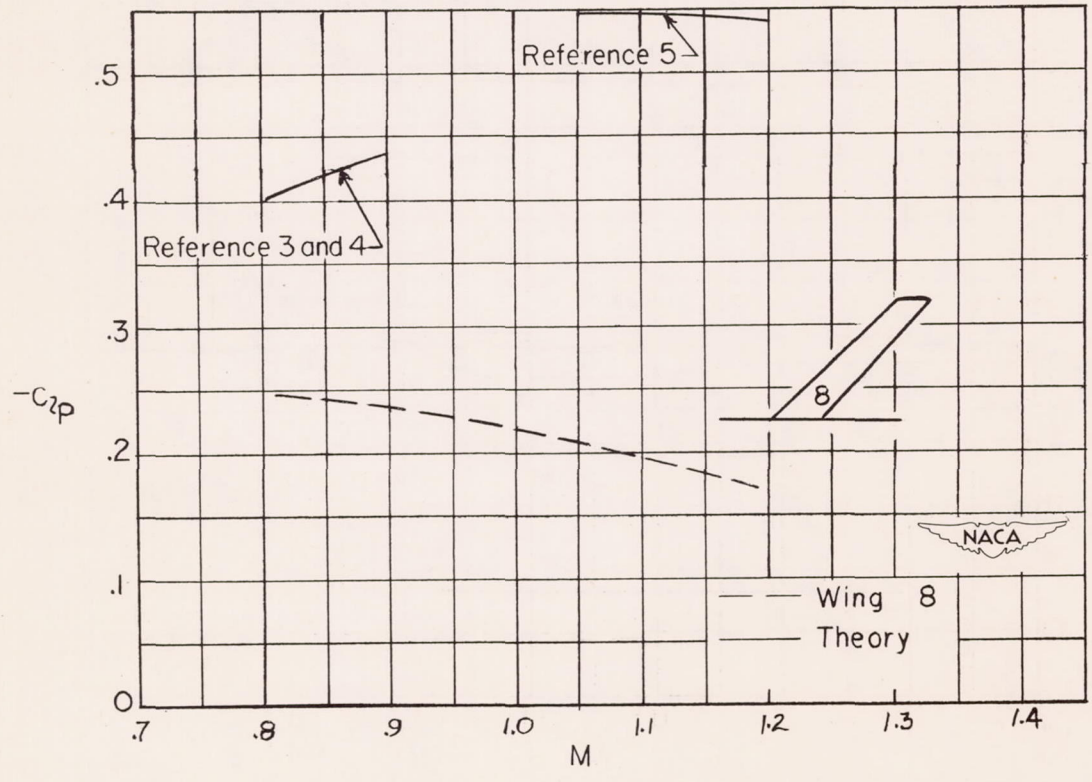

(f) NACA 65A009 airfoil. $\Lambda = 46.2^{\circ}$.

Figure 4.- Concluded.

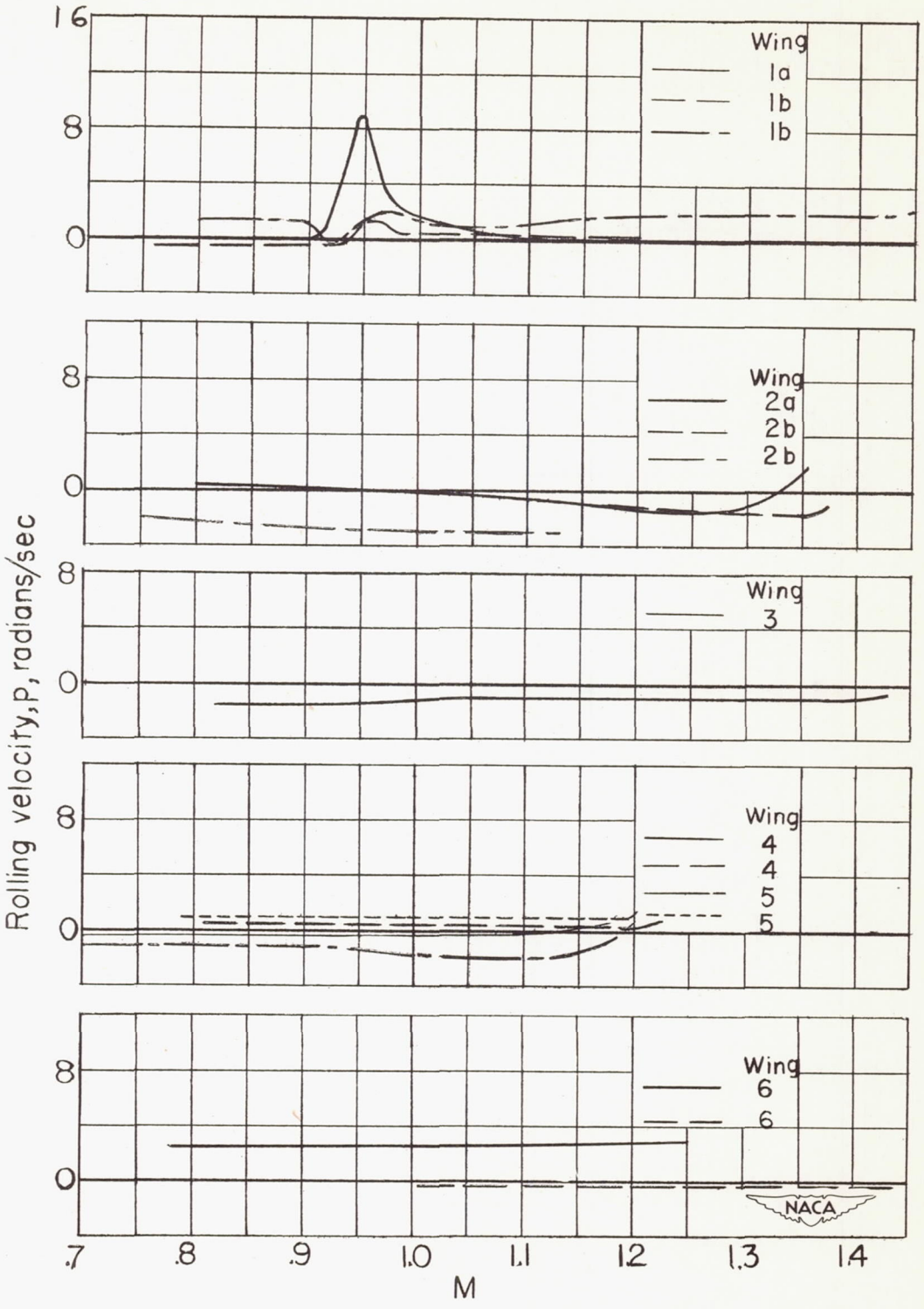

(a) Wings 1 to 6.

Figure 5.- Variation of rolling velocity with Mach number in coasting flight.

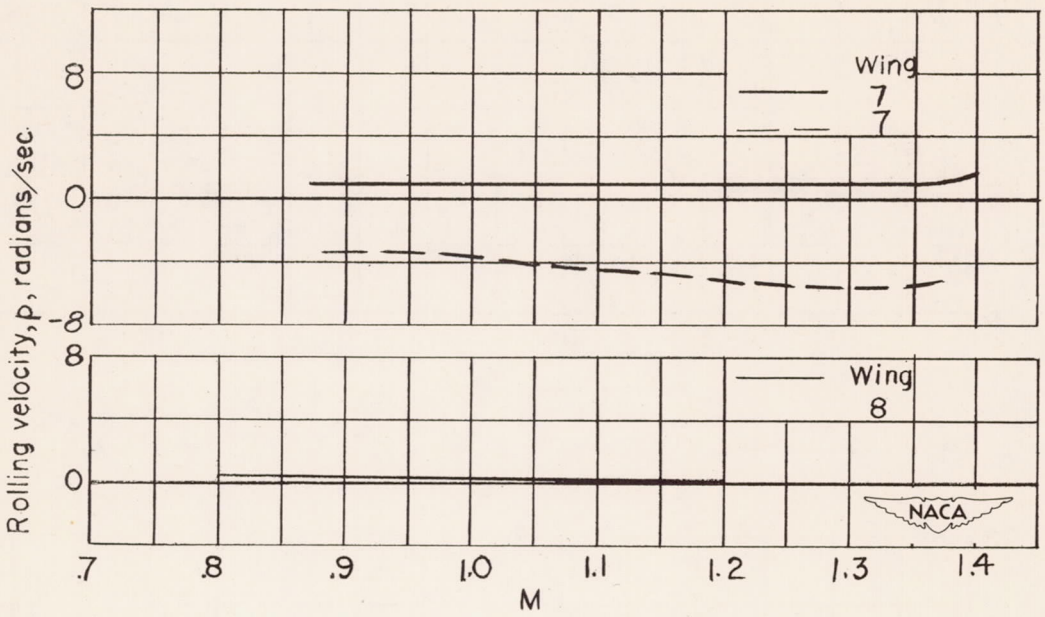

(b) Wings 7 and 8.

Figure 5.- Concluded.

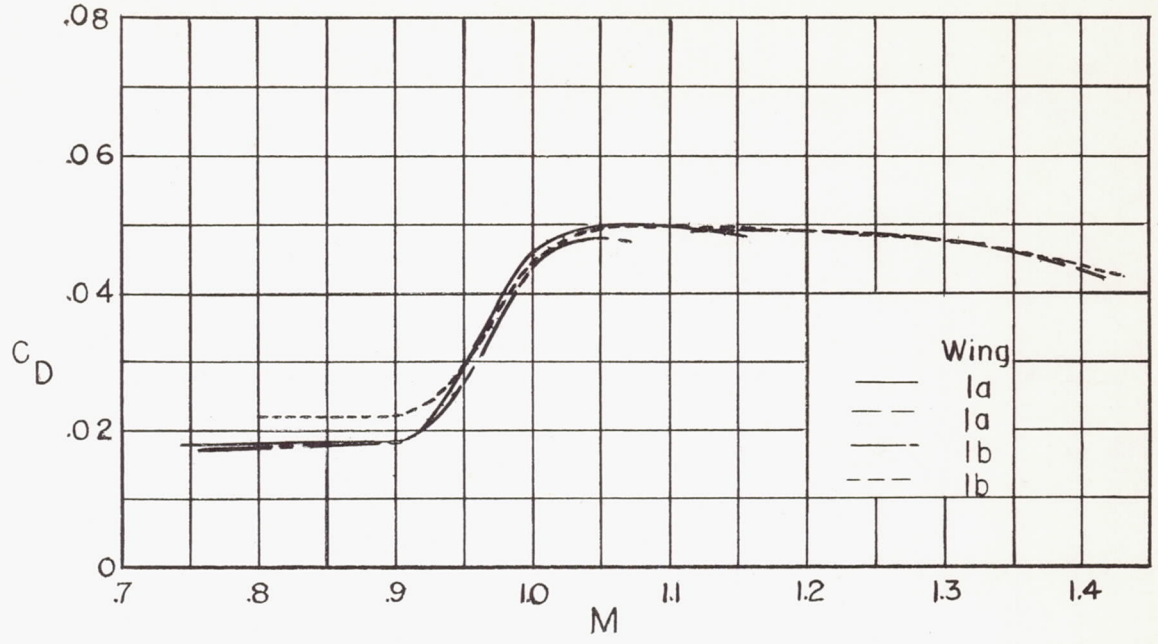

(a) Circular-arc airfoil. $\Lambda = 42.7^{\circ}$; A = 4.0; $\lambda = 0.5$; $\frac{t}{c} = 0.10$.

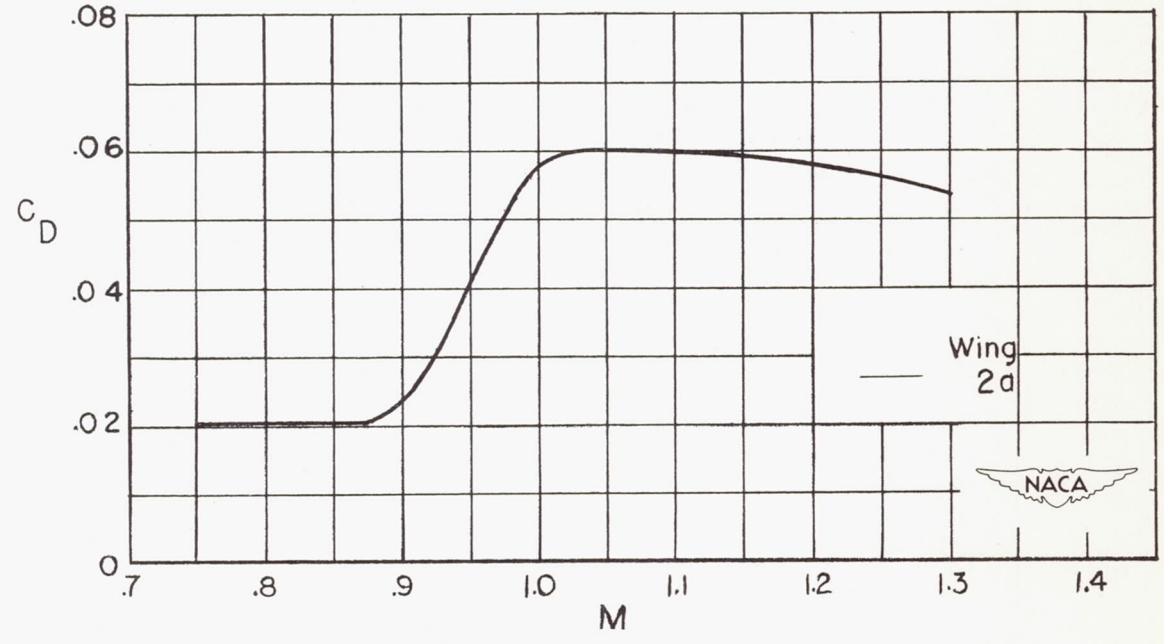

(b) NACA 63-series airfoil. $\Lambda = 36.5^{\circ}$; A = 3.5; $\lambda = 0.56$; $\frac{t}{c} = 0.10$ to 0.12.

Figure 6.- Variation of total drag coefficient with Mach number.

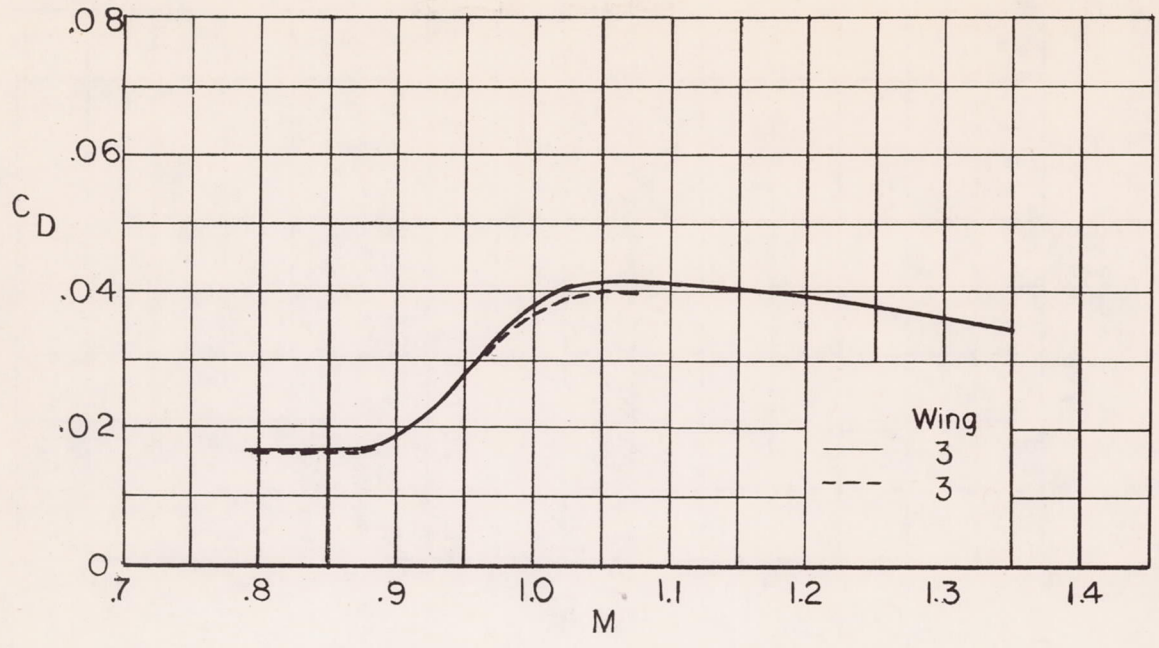

(c) Hexagonal airfoil. $\Lambda = 23.1^{\circ}$; A = 2.9; $\lambda = 0.41$; $\frac{t}{c} = 0.045$.

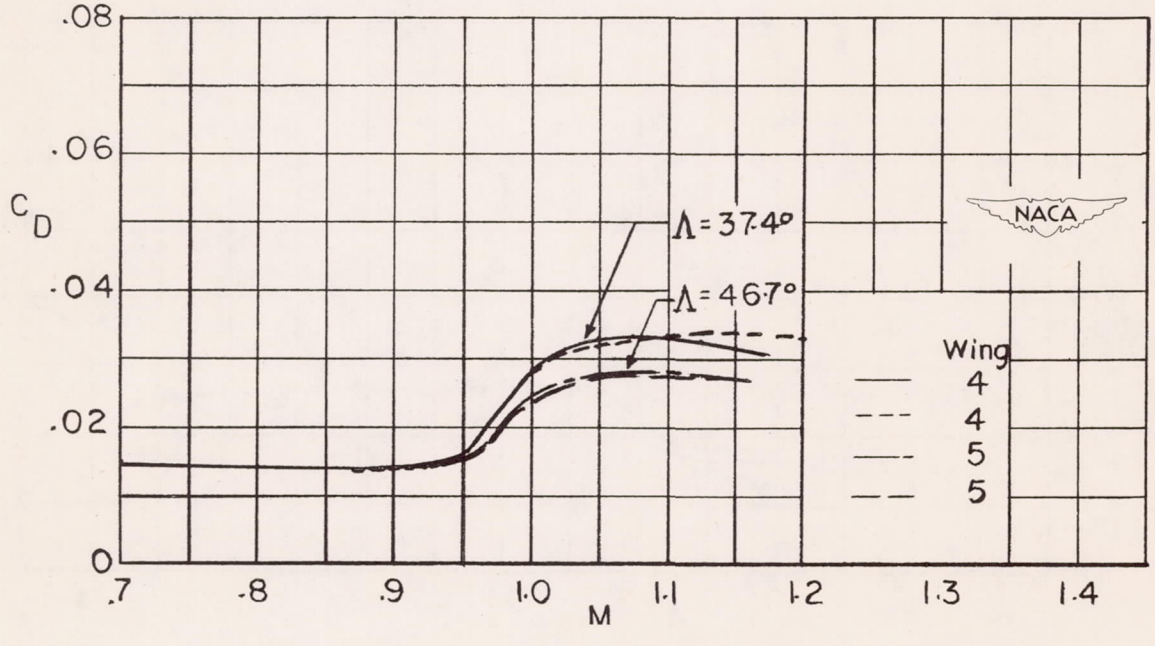

(d) NACA 65A006 airfoil. A = 4.0; $\lambda = 0.6$; $\frac{t}{c} = 0.06$.

Figure 6.- Continued.

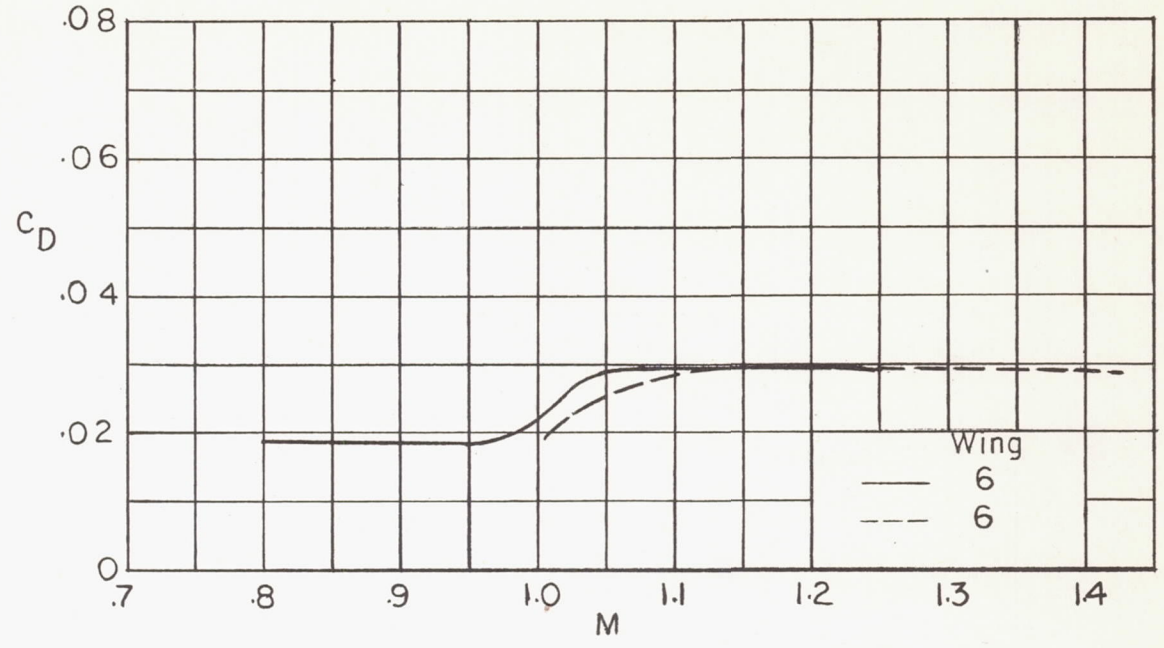

(e) NACA 65A006 airfoil. $\Lambda = 60.9^{\circ}$; $A = 4.0$; $\lambda = 0.60$; $\frac{t}{c} = 0.06$.

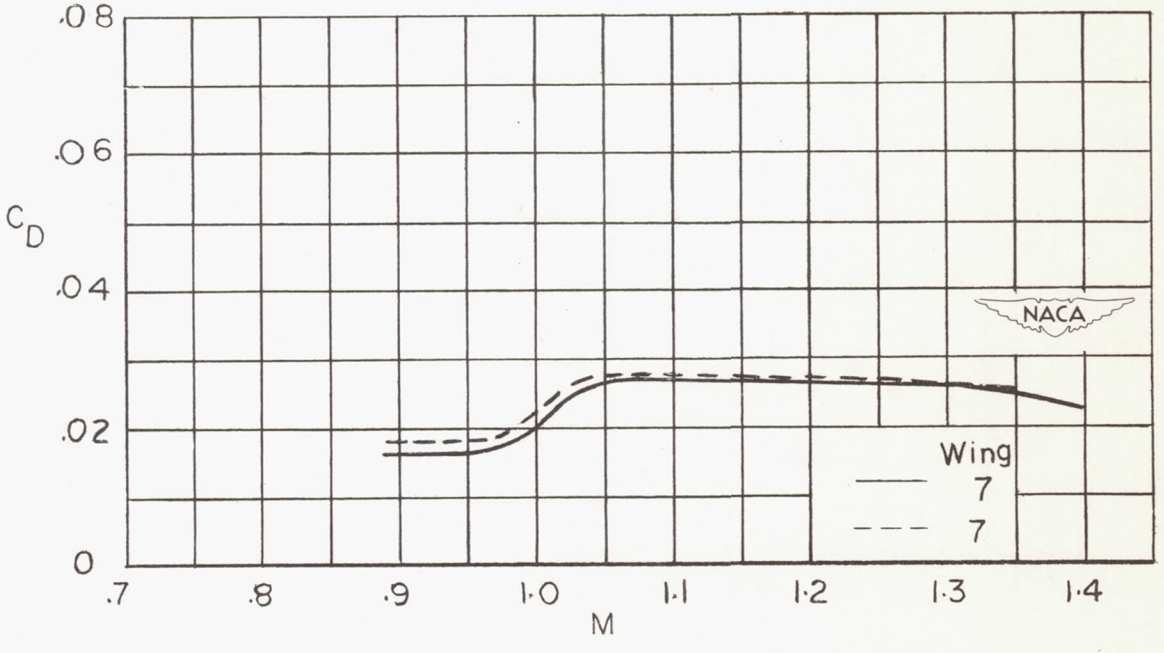

(f) NACA 64A005 airfoil. $\Lambda = 63.0^{\circ}$; $A = 3.5$; $\lambda = 0.25$; $\frac{t}{c} = 0.05$.

Figure 6.- Continued.

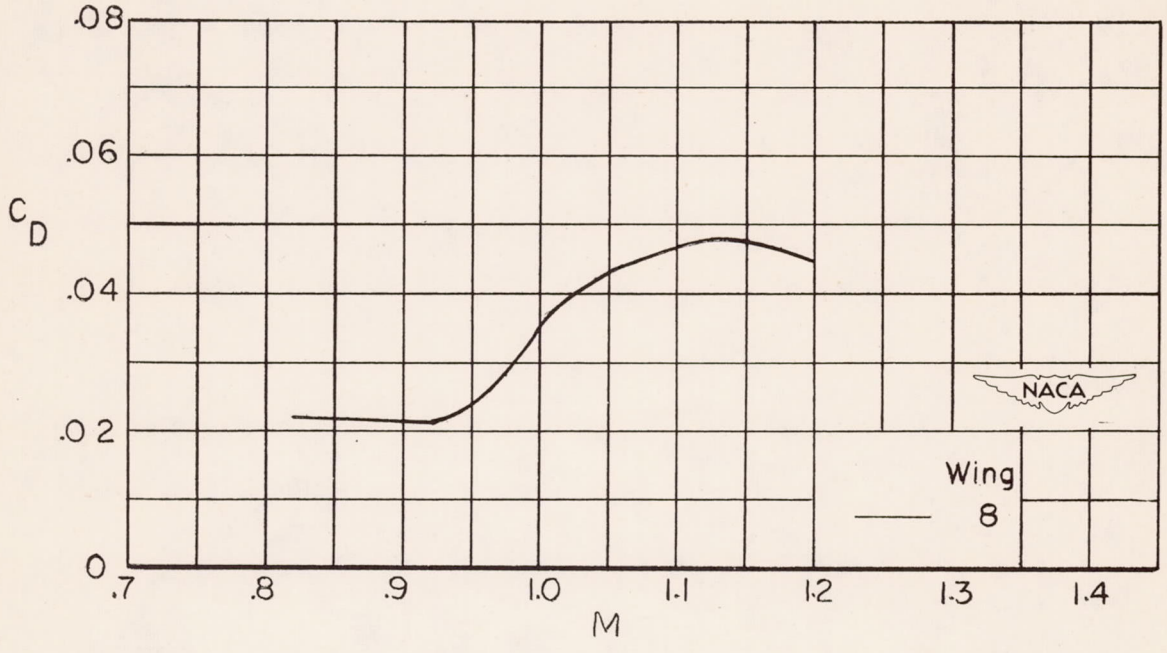

(g) NACA 65A009 airfoil. $\Lambda = 46.2^{\circ}$; $A = 6.0$; $\lambda = 0.60$; $\frac{t}{c} = 0.09$.

Figure 6.- Concluded.